Int. J. Heat Mass Transfer. Vol. 36, No. 17, pp. 4221–4231, 1993
Printed in Great Britain

0017–9310/93 $6.00 + 0.00

Stationary and dynamic simulation of multipass shell and tube heat exchangers with the dispersion model for both fluids

YIMIN XUAN
Nanjing University of Science and Technology, 200 Xiao Ling Wei, Nanjing 210014, China

and

WILFRIED ROETZEL
Institute of Thermodynamics, University of the Federal Armed Forces Hamburg, D-22039 Hamburg, Germany

(*Received* 16 *April* 1993)

Abstract—The dispersion model is applied to the description of the effects of shell and tubeside flow maldistribution. By means of this model, an efficient and versatile method of predicting transient response of multipass shell and tube heat exchangers is developed. The method allows for effect of maldistribution on transient process, influence of heat capacities of fluids and solid components, arbitrary inlet temperature variations and step disturbances of flow rates. General forms of initial conditions and two different flow arrangements are considered. A general form of the solution for steady-state and dynamic simulation is derived. Temperature profiles are determined with numerical inversion of the Laplace transform. Some examples are calculated and the effect of maldistribution is discussed.

1. INTRODUCTION

THE TRANSIENT performance of a shell and tube heat exchanger mainly results from inlet temperature and flow variations. Such disturbances may occur on both shell and tube sides simultaneously or separately. There are plenty of published papers which separated the above-mentioned two types of inlet changes. They were engaged either on responses to inlet temperature changes [1, 2] or to flow variations [3, 4]. Stainthorp and Axon [5] described the dynamic behaviour of multipass heat exchangers subject to steam temperature and steam flow perturbations by the modified one-pass model. Forghieri and Papa [6] set up three different models of a counterflow heat exchanger with temperature disturbances and step flow variations and obtained the asymptotic solution to step variations of the flow rate by means of the Laplace transform. All these works are based on the conventional plug-flow model, i.e. no dispersion (or backmixing) occurs in the flow direction and the axial velocity of process fluid is uniform. Xuan and Roetzel [7] applied the shellside dispersion model to predicting dynamic response to both arbitrary temperature changes and step flow variations in parallel and counterflow heat exchangers and showed good agreement between the theoretical and experimental results. However, only the shellside flow maldistribution was involved.

Generally, flow maldistribution can take place on both shell and tube sides. The complicated shellside geometrical structure and manufacturing clearances induce non-uniform distributions of fluid such as leakage, bypass and backmixing [8]. On the other hand, the tubeside fluid may not be evenly distributed among parallel channels in a pass because of different pressure drops in channels which is more severe for laminar flow. For fixed-tubesheet or floating-head type exchangers, the tubeside fluid is stirred in the headers and this effect on stationary and transient process cannot be described by the plug-flow model. In general, poor flow distribution causes degradation in performance of exchangers, especially for exchangers with greater number of heat transfer units *NTU*.

Based on the dispersion model rather than the ideal plug-flow model, in the present paper a new method is developed to predict transient behaviour of multipass shell and tube heat exchangers subject to arbitrary temperature variations and step flow disturbances with regard to shell and tubeside maldistributions. In order to provide a versatile solution, the derivation involves the influence of heat capacities of both fluids and the capacities of shell and tube wall. Two different flow arrangements and arbitrary number and different size of tube passes are included. In addition, non-zero initial conditions are allowed. The Laplace transform is used to convert partial differential equations into ordinary differential equations and the temperature profiles in time domain are obtained by means of numerical inversion.

2. MATHEMATICAL FORMULATION

The following assumptions are necessary for modelling transient process of multipass shell and tube heat exchangers:

NOMENCLATURE

A	heat transfer surface area [m^2]
A_q	transverse area of flow [m^2]
C	heat capacity [J K^{-1}]
coef	ratio of U_s to U_1, U_s/U_1
D	dispersion coefficient or apparent heat conductivity [W m^{-1} K^{-1}]
$f_1(z), f_2(z)$	inlet temperature changes
$F_1(s), F_2(s)$	transformed forms of $f_1(z)$ and $f_2(z)$ in the image domain
$g_i(x)$	initial conditions defined in equation (11)
h	heat transfer coefficient [W m^{-2} K^{-1}]
I	flow arrangement I, as shown in Fig. 1
II	flow arrangement II, as shown in Fig. 1
l	distance of flow from the entrance of shellside fluid [m]
L	total length of flow path [m]
N	number of tubeside passes
NTU	number of transfer units [dimensionless]
Pe	Péclet number defined in equations (7) and (8)
s	parameter of the Laplace transform
t	dimensionless temperature, $(\theta-\theta_{r2})/(\theta_{r1}-\theta_{r2})$
$\dot{W}$	thermal flow rate (heat capacity flow rate) [W K^{-1}]
x	dimensionless space coordinate, l/L
z	dimensionless time, τ/τ_{r1}.

Greek symbols

β	eigenvalues
θ	temperature [K]
θ_r	reference temperature [K]
λ	heat conductivity [W m^{-1} K^{-1}] also eigenvalues
σ	ratio of flow rates before and after a step flow disturbance
τ	time [s]
τ_r	residence time of fluid in the heat exchanger [s].

Subscripts

0	initial state
1	shellside fluid
2	tubeside fluid
e	exit
s	shell
w	tube wall.

Subscript

′	inlet
″	exit.

(1) All thermal properties are constant.

(2) The heat transfer coefficient is constant within any tubeside pass, but it may vary from pass to pass.

(3) The effect of maldistribution can be described by a dispersion term in the energy equation.

(4) The tube wall possesses the infinite and zero heat conductivity normal and parallel to the flow direction, respectively.

(5) The outside shell surface is adiabatic from the environment.

The scheme of multipass shell and tube heat exchangers (designated as $1-N$) is shown in Fig. 1, where the origin-point of the coordinate system is always located at the entrance of shellside fluid. Instead of the ideal plug-flow model, one applies the dispersion model to deriving the governing differential equations. For this purpose, auxiliary variables $\tilde{t}_1$ and $\tilde{t}_{2i}$ $(i = 1, 2, \ldots, N)$ are introduced as follows:

$$\dot{W}_1\tilde{t}_1 = \dot{W}_1\theta_1 - LA_{q1}D_1\frac{\partial\theta_1}{\partial l},$$

$$\dot{W}_{2i}\tilde{t}_{2i} = \dot{W}_{2i}\theta_{2i} \pm (-1)^i LA_{q2i}D_{2i}\frac{\partial\theta_{2i}}{\partial l}. \quad (1)$$

In these two expressions the first term on the right side corresponds to the convective part and the second term the dispersion part. Therefore, the governing equations are written:

$$A_{q1}D_1\frac{\partial^2\theta_1}{\partial l^2} - \dot{W}_1\frac{\partial\theta_1}{\partial l} - \frac{C_1}{L}\frac{\partial\theta_1}{\partial\tau} - \sum_{i=1}^{N}\frac{(hA)_{1i}}{L}(\theta_1-\theta_{wi}) - \frac{(hA)_s}{L}(\theta_1-\theta_s) = 0 \quad (2)$$

$$A_{q2i}D_{2i}\frac{\partial^2\theta_{2i}}{\partial l^2} \pm (-1)^i\dot{W}_{2i}\frac{\partial\theta_{2i}}{\partial l} - \frac{C_{2i}}{L}\frac{\partial\theta_{2i}}{\partial\tau} - \frac{(hA)_{2i}}{L}(\theta_{2i}-\theta_{wi}) = 0 \quad (i = 1, 2, \ldots, N) \quad (3)$$

where the positive sign $(+)$ and the negative $(-)$ of $(\pm)$ in equation (3) are valid for flow arrangement II and flow arrangement I, respectively. With respect to influence of heat capacities of shell and tube walls, the corresponding energy equations are as follows:

$$C_s\frac{\partial\theta_s}{\partial\tau} - (hA)_s(\theta_1-\theta_s) = 0 \quad (4)$$

$$C_w\frac{\partial\theta_{wi}}{\partial\tau} - (hA)_{1i}(\theta_1-\theta_{wi}) - (hA)_{2i}(\theta_{2i}-\theta_{wi}) = 0 \quad (i = 1, 2, \ldots, N). \quad (5)$$

In equations (4) and (5) no axial conduction term exists since it may be neglected according to separate calculations [9]. The coefficient D appearing in equations (1)–(3) is called the axial (or longitudinal) dispersion coefficient (or apparent heat conductivity).

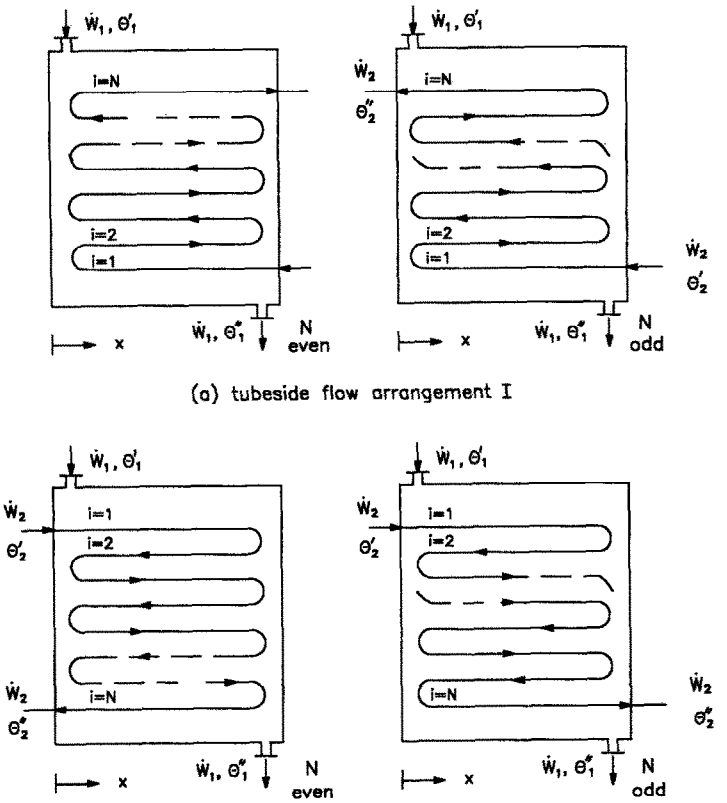

FIG. 1. Schematic representation of multipass shell and tube heat exchangers.

As a matter of fact, it consists of the following two parts : the heat conductivity λ_f of fluid and the eddy diffusion coefficient D_f caused by flow maldistribution, i.e. $D = D_f + \lambda_f$. If the flow is pure plug flow and no eddy diffusion occurs, $D_f = 0$. C_1 represents the total heat capacity of the shellside fluid which includes both the fluid part within the tube bundle and that between the bundle and the shell, C_{2i} the heat capacity of the tubeside fluid remaining in tube pass i and inside the corresponding headers (if the fixed-tubesheet type or the floating-header type of tubeside construction is used), and C_{wi} the heat capacity of the wall of tube pass i. With regard to baffles and end plates, one can approximately distribute the heat capacities of these components among all tube passes. In this case, C_{wi} is replaced by

$$C^*_{wi} = C_{wi}(1+\gamma_i) \tag{6}$$

where C^*_{wi} is the apparent heat capacity of tube pass i and γ_i a parameter for solid components such as baffles and end plates. The value of γ_i may vary with tube pass. Thus, the influence of these components on transient performance of heat exchangers can be taken into account. If this influence is negligible, $\gamma_i = 0$. For simplicity, the asterisk '*' is omitted in the following analysis. The thermal flow rate $\dot{W}_{2i}$ does not change from pass to pass, but the heat capacity C_{2i} may be different among tube passes according to the given geometric dimension of exchangers. To facilitate further derivation, residence times τ_{r1}, τ_{r2} and some parameters are defined as follows :

$$\tau_{r1} = \frac{C_1}{\dot{W}_1}, \quad \tau_{r2} = \frac{C_2}{\dot{W}_2}, \quad \tau_{r2i} = \frac{C_{2i}}{\dot{W}_{2i}},$$

$$R_1 = \frac{\dot{W}_1}{\dot{W}_2} = \frac{1}{R_2},$$

$$NTU_1 = \frac{1}{\dot{W}_1}\left[\frac{1}{(hA)_1} + \frac{1}{(hA)_2}\right]^{-1} = \frac{U_1 U_2 R_2}{U_1 + U_2 R_2}$$

$$U_1 = \frac{(hA)_1}{\dot{W}_1}, \quad U_2 = \frac{(hA)_2}{\dot{W}_2}, \quad U_{1i} = \frac{(hA)_{1i}}{\dot{W}_1},$$

$$U_{2i} = \frac{(hA)_{2i}}{\dot{W}_2}, \quad U_s = \frac{(hA)_s}{\dot{W}_1}, \quad \varepsilon_{1i} = \frac{(hA)_{1i}}{(hA)_1} = \frac{U_{1i}}{U_1},$$

$$\varepsilon_{2i} = \frac{(hA)_{2i}}{(hA)_2} = \frac{U_{2i}}{U_2}, \quad \varepsilon_{ci} = \frac{C_{2i}}{C_2}, \quad \varepsilon_{wi} = \frac{C_{wi}}{C_w}$$

where

$$(hA)_1 = \sum_{i=1}^{N} (hA)_{1i}, \quad (hA)_2 = \sum_{i=1}^{N} (hA)_{2i},$$

$$C_2 = \sum_{i=1}^{N} C_{2i} \quad \text{and} \quad C_w = \sum_{i=1}^{N} C_{wi}.$$

Obviously, there are the following relationships :

$$\sum_{i=1}^{N} \varepsilon_{1i} = 1, \quad \sum_{i=1}^{N} \varepsilon_{2i} = 1, \quad \sum_{i=1}^{N} \varepsilon_{ci} = 1,$$

$$\sum_{i=1}^{N} \varepsilon_{wi} = 1 \quad \text{and} \quad \tau_{r2i} = \varepsilon_{ci}\tau_{r2}.$$

The other dimensionless parameters are defined as

$$R_\tau = \frac{\tau_{r2}}{\tau_{r1}}, \quad R_{c1} = \frac{C_1}{C_2} = \frac{R_1}{R_\tau} = \frac{1}{R_{c2}},$$

$$R_w = \frac{C_w}{C_1 + C_2}, \quad R_{wi} = \frac{C_{wi}}{C_1 + C_2}, \quad R_s = \frac{C_s}{C_w},$$

$$\alpha_{1i} = \frac{U_{1i}}{1 + R_{c2}}, \quad \alpha_{2i} = \frac{U_{2i}}{R_\tau(1 + R_{c1})}.$$

Insertion of the dimensionless space variable $x = l/L$, the dimensionless time $z = \tau/\tau_{r1}$, the dimensionless temperature $t = (\theta - \theta_{r2})/(\theta_{r1} - \theta_{r2})$ and the above-defined parameters into equations (1), (3), (4) and (5) yields :

$$\frac{1}{Pe_1}\frac{\partial^2 t_1}{\partial x^2} - \frac{\partial t_1}{\partial x} - \frac{\partial t_1}{\partial z} - \sum_{i=1}^{N} U_{1i}(t_1 - t_{wi}) - U_s(t_1 - t_s) = 0 \quad (7)$$

$$\frac{1}{Pe_{2i}}\frac{\partial^2 t_{2i}}{\partial x^2} \pm (-1)^i \frac{\partial t_{2i}}{\partial x} - \varepsilon_{ci} R_\tau \frac{\partial t_{2i}}{\partial z} - U_{2i}(t_{2i} - t_{wi}) = 0 \quad (8)$$

$$R_{wi}\frac{\partial t_{wi}}{\partial z} - \alpha_{1i}(t_1 - t_{wi}) - \alpha_{2i}(t_{2i} - t_{wi}) = 0 \quad (9)$$

$$R_s R_w (1 + R_{c2})\frac{\partial t_s}{\partial z} - U_s(t_1 - t_s) = 0 \quad (10)$$

where Pe is the Péclet number whose definition is given by $Pe = \dot{W}L/A_q D$. It quantitatively describes the efffect of maldistribution on transient behaviour. For plug flow $D = 0$ (heat conduction in fluid is generally negligible) and $Pe \to \infty$, so that equations (7)–(10) are reduced to the same form derived by the ideal plug-flow model [10]. The actual flow pattern in heat exchangers interposes between axially unmixed plug flow and perfect axial mixing and the value of Pe lies in the range $0 < Pe < \infty$. The general forms of initial temperatures are expressed by

$$t_1(x,0) = g_1(x), \quad t_s(x,0) = g_s(x)$$

$$t_{2i}(x,0) = g_{2i}(x), \quad t_{wi}(x,0) = g_{wi}(x)$$

$$(i = 1, 2, \ldots, N). \quad (11)$$

All these functions are dependent on the temperature distributions at the instant of a new transient process. Equating the heat flux due to convention just outside the entrance (or exit) of heat exchangers with that due to convection and dispersion just inside the entrance (or exit) of heat exchangers [11], one obtains the suitable boundary conditions pertinent to the dispersion model. The shellside boundary conditions are :

$$t_1 - \frac{1}{Pe_1}\frac{\partial t_1}{\partial x} = f_1(z) \quad \text{at } x = 0$$

and

$$\frac{\partial t_1}{\partial x} = 0 \quad \text{at } x = 1. \quad (12)$$

Similarly, one has the following tubeside boundary conditions. For flow arrangement I :

$$t_{21} + \frac{1}{Pe_{21}}\frac{\partial t_{21}}{\partial x} = f_2(z) \quad \text{at } x = 1$$

and

$$\frac{\partial t_{2N}}{\partial x} = 0 \quad \text{at } x = 0 \text{ (odd } N\text{)} \quad \text{or at } x = 1 \text{ (even } N\text{)} \quad (13)$$

and for flow arrangement II :

$$t_{21} - \frac{1}{Pe_{21}}\frac{\partial t_{21}}{\partial x} = f_2(z) \quad \text{at } x = 0$$

and

$$\frac{\partial t_{2N}}{\partial x} = 0 \quad \text{at } x = 0 \text{ (even } N\text{)} \quad \text{or at } x = 1 \text{ (odd } N\text{)} \quad (14)$$

where $f_1(z)$ and $f_2(z)$ indicate any arbitrary shell and tubeside inlet temperature variations, respectively. These changes may take place simultaneously or separately. The other $(2N-2)$ necessary conditions are interface conditions between adjacent tube passes at location $x = 0$ and $x = 1$. They are listed in Table 1 in which $t_{2i,i+1}$ represents the intermediate temperature of the tubeside fluid between two adjacent passes.

If step disturbance of flow rates occurs, derivation becomes somewhat complicated. Using the subscript '0' to express the initial state before the step change, one defines $\sigma_1 = u_1/u_{10}$ and $\sigma_2 = \sigma_{2i} = u_{2i}/u_{2i0}$. If flow patterns remain the same, i.e. laminar or turbulent before and after the disturbance, the heat transfer coefficient h_1 and h_{2i} can be expressed as

$$h_1 = \sigma_1^{n_1} h_{10} \quad \text{and} \quad h_{2i} = \sigma_{2i}^{n_2} h_{2i0} \quad (15)$$

where the exponent n_1 depends upon the value of the Reynolds number, the geometric characteristics and the arrangement of tube bank. The average value is $n_1 = 0.63$ for in-line bank and $n_1 = 0.6$ for staggered bank in the range $10^3 < Re_1 < 2 \times 10^5$. The exponent n_2 depends upon the flow pattern in tubes and $n_2 = 0.8$ for fully developed turbulent flow in a smooth circular tube. The thermal flow rates $\dot{W}_1$, $\dot{W}_{2i}$ and other afore-defined parameters are rewritten as follows :

$$\dot{W}_1 = \dot{W}_{10}\sigma_1, \quad \dot{W}_2 = \dot{W}_{20}\sigma_2$$

$$\tau_{r1} = \frac{\tau_{r10}}{\sigma_1}, \quad \tau_{r2} = \frac{\tau_{r20}}{\sigma_2}$$

$$R_\tau = R_{\tau 0}\frac{\sigma_1}{\sigma_2}, \quad R_1 = R_{10}\frac{\sigma_1}{\sigma_2}$$

$$U_1 = U_{10}\sigma_1^{n_1 - 1}, \quad U_2 = U_{20}\sigma_2^{n_2 - 1}.$$

Table 1. The interface conditions for $t_2(x,z)$

	$x=0,\quad z\geqslant 0$	$x=1,\quad z\geqslant 0$
	$t_{2i}=t_{2i+1}=t_{2i,i+1}$	$t_{2i}=t_{2i+1}=t_{2i,i+1}$
	$\frac{1}{Pe_{2i}}\frac{\partial t_{2i}}{\partial x}=-\frac{1}{Pe_{2i+1}}\frac{\partial t_{2i+1}}{\partial x}$	$\frac{1}{Pe_{2i}}\frac{\partial t_{2i}}{\partial x}=-\frac{1}{Pe_{2i+1}}\frac{\partial t_{2i+1}}{\partial x}$
	even N	
I	$i=1,3,\ldots,N-1$	$i=2,4,\ldots,N-2$
II	$i=2,4,\ldots,N-2$	$i=1,3,\ldots,N-1$
	odd N	
I	$i=1,3,\ldots,N-2$	$i=2,4,\ldots,N-1$
II	$i=2,4,\ldots,N-1$	$i=1,3,\ldots,N-2$

If there are only temperature changes at inlets, $\sigma_1=\sigma_2=1$ and all the above-mentioned parameters are constant; otherwise $\sigma_1\neq 1$ and $\sigma_2\neq 1$. For $(2N+2)$ partial differential equations (7)–(10), the Laplace transform is used to reduce the number of the equations. Using s as the Laplace parameter with respect to the dimensionless time z, one obtains the following transformed equations under the general initial conditions (11):

$$\frac{d^2T_1}{dx^2}-Pe_1\frac{dT_1}{dx}=Pe_1\left(s+U_1+U_s-\sum_{i=1}^{N}\frac{\varepsilon_{1i}\alpha_{1i}U_1}{\alpha_{1i}+\alpha_{2i}+R_{wi}s}-\frac{U_s^2}{R_sR_w(1+R_{c2})s+U_s}\right)T_1-Pe_1\sum_{i=1}^{N}\frac{\varepsilon_{1i}\alpha_{2i}U_1}{\alpha_{1i}+\alpha_{2i}+R_{wi}s}T_{2i}+h_1(x) \quad (16)$$

$$\frac{d^2T_{2i}}{dx^2}\pm(-1)^i Pe_{2i}\frac{dT_{2i}}{dx}=-\frac{Pe_{2i}\varepsilon_{2i}\alpha_{1i}U_2}{\alpha_{1i}+\alpha_{2i}+R_{wi}s}T_1-Pe_{2i}\left(\frac{\varepsilon_{2i}\alpha_{2i}U_2}{\alpha_{1i}+\alpha_{2i}+R_{wi}s}-\varepsilon_{ci}R_\tau s-\varepsilon_{2i}U_2\right)T_{2i}+h_{2i}(x)\quad (i=1,2,\ldots,N) \quad (17)$$

$$T_{wi}=\frac{\alpha_{1i}T_1+\alpha_2T_{2i}}{\alpha_{1i}+\alpha_{2i}+R_{wi}s}+h_{wi}(x)\quad (i=1,2,\ldots,N) \quad (18)$$

$$T_s=\frac{U_sT_1}{R_sR_w(1+R_{c2})s+U_s}+h_s(x) \quad (19)$$

where

$$h_1(x)=-Pe_1\left[g_1(x)+\sum_{i=1}^{N}\frac{U_1R_{wi}}{\alpha_{1i}+\alpha_{2i}+R_{wi}s}g_{wi}(x)+\frac{U_sR_sR_w(1+R_{c2})}{U_s+R_sR_w(1+R_{c2})s}g_s(x)\right],$$

$$h_{2i}(x)=-Pe_{2i}\left[\varepsilon_{ci}R_\tau g_{2i}(x)+\frac{U_{2i}R_{wi}}{\alpha_{1i}+\alpha_{2i}+R_{wi}s}g_{wi}(x)\right],$$

$$h_{wi}(x)=\frac{R_{wi}}{\alpha_{1i}+\alpha_{2i}+R_{wi}s}g_{wi}(x),$$

$$h_s(x)=\frac{R_sR_w(1+R_{c2})}{U_s+R_sR_w(1+R_{c2})s}g_s(x).$$

By introducing the following variables

$$\tilde{T}_1=\frac{dT_1}{dx}\quad\text{and}\quad\tilde{T}_{2i}=\frac{dT_{2i}}{dx}\quad(i=1,2,\ldots,N),$$

equations (16) and (17) are replaced by $(2N+2)$ first-order differential equations which are expressed in matrix notation

$$\frac{d\mathbf{T}}{dx}=\mathbf{AT}+\mathbf{H}(x) \quad (20)$$

where vector

$$\mathbf{T}=(T_{21},T_{22},\ldots,T_{2N},\tilde{T}_{21},\tilde{T}_{22},\ldots,\tilde{T}_{2N},T_1,\tilde{T}_1)^{\mathrm{T}}$$

and

$$\mathbf{H}(x)=[0,0,\ldots,h_{21}(x),h_{22}(x),\ldots,h_{2N}(x),0,h_1(x)]^{\mathrm{T}}$$

and $\mathbf{A}$ is a $(2N+2)\times(2N+2)$ matrix whose elements are given by equations (16) and (17). Since $\mathbf{A}$ is a constant matrix, one is able to find the closed solution to equation (20). With $(2N+2)$ eigenvalues $\{\beta_j\}$ $(j=1,2,\ldots,2N+2)$ of $\mathbf{A}$ and the corresponding eigenvectors $\{\mathbf{u}_j\}$, one can build the solution to equation (20), although equation (20) is a boundary value problem rather than an initial value problem. A general form of the solution yields

$$\mathbf{T}=e^{Ax}\mathbf{D}^*+e^{Ax}\int e^{-Ax'}\mathbf{H}(x')\,dx'. \quad (21)$$

Since $e^{Ax}=\mathbf{U}e^{Bx}\mathbf{U}^{-1}$ and $e^{Ax}\mathbf{D}^*$ can be always converted into $\mathbf{U}e^{Bx}\mathbf{D}$, one has

$$\mathbf{T}=\mathbf{U}e^{Bx}\mathbf{D}+\int\mathbf{U}e^{B(x-x')}\mathbf{U}^{-1}\mathbf{H}(x')\,dx' \quad (22)$$

where e^{Bx} is a diagonal matrix, i.e.

$$e^{Bx}=\mathrm{diag}\{e^{\beta_1x},e^{\beta_2x},\ldots,e^{\beta_{2N+2}x}\},$$

$\mathbf{U}$ is a $(2N+2)\times(2N+2)$ matrix whose columns are

the corresponding eigenvectors, i.e. $\mathbf{U} = \{\mathbf{u}_1, \mathbf{u}_2, \ldots, \mathbf{u}_{2N+2}\}$ and $\mathbf{D}$ (or $\mathbf{D}^*$) is a coefficient vector which must be determined according to the boundary conditions. The necessary condition of solution (21) or (22) is that all eigenvalues are distinct. In general, the eigenvalues of $\mathbf{A}$ in equation (20) describing transient behaviour of multipass shell and tube heat exchangers are different from each other. If there exist some eigenvalues of multiplicity m ($m > 1$), one must build anew the solution to equation (20) and it is a somewhat awkward task. An approximation method can avoid such a difficulty. Introducing an infinitesimal parameter δ (for example $\delta = 10^{-4}$), one changes the value of ε_i by adding or decreasing δ under the constraint $\sum \varepsilon_i = 1$, so that one may have distinct eigenvalues again. Such a slight change of ε_i causes almost no changes of calculated temperature profiles and the overall accuracy is not affected.

Insertion of the boundary conditions (12)–(14) and the interface conditions listed in Table 1 into equation (22) leads to the following matrix equation

$$\mathbf{WD} = \mathbf{F} + \mathbf{S} \tag{23}$$

where $\mathbf{W}$ is a $(2N+2)\times(2N+2)$ matrix whose elements are prescribed by the aforementioned determinant conditions. It varies with number N of tube passes as well as flow arrangement. Vector $\mathbf{F} = [0, 0, \ldots, F_2(z), F_1(z)]^{\mathrm{T}}$ if the inlet conditions are placed in the last two rows of matrix equation (23), and vector $\mathbf{S} = (s_1, s_2, \ldots, s_{2N+2})^{\mathrm{T}}$ is determined by the second term on the right side of equation (22), i.e. $s_i = 0$ or s_i takes the integration value from $x = 0$ to 1. The position of s_i in vector $\mathbf{S}$ corresponds to arrangement order of matrix $\mathbf{W}$. Therefore, the coefficient vector $\mathbf{D}$ follows

$$\mathbf{D} = \mathbf{W}^{-1}(\mathbf{F} + \mathbf{S}). \tag{24}$$

So far the transformed temperature profiles and temperature gradients of both fluids in the Laplace image domain have been found. Their explicit expressions are

$$T_i(x,s) = \sum_{j=1}^{2N+2} d_j u_{ij} \mathrm{e}^{\beta_j x} + \sum_{k=1}^{2N+2} \sum_{j=1}^{2N+2} u_{ij} v_{jk} \int \mathrm{e}^{\beta_j (x-x')} h_k(x')\,\mathrm{d}x' \qquad (i = 1, 2, \ldots, 2N+2) \tag{25}$$

where d_j, u_{ij}, v_{jk} and $h_k(x)$ are elements of $\mathbf{D}$, $\mathbf{U}$, $\mathbf{U}^{-1}$ and $\mathbf{H}(x)$, respectively. From expression (25), one can easily determine the transformed responses at exits. The related profiles in tube walls and shell are already given by equations (18) and (19).

3. INITIAL CONDITIONS

Function $h_k(x)$ in equation (25) consists of initial temperature distributions $g_1(x)$, $g_s(x)$, $g_{2i}(x)$ and $g_{wi}(x)$. These temperature distributions may appear in different forms according to the instant state of transient process. Three typical forms of the initial temperature profiles are described as follows.

(1) *Uniform initial conditions*

This kind of initial conditions is the simplest case. Zero conditions $g_1(x) = g_s(x) = 0$ and $g_{2i}(x) = g_{wi}(x) = 0$ make equation (20) homogeneous and its general solution is

$$\mathbf{T} = \mathbf{U}\,\mathrm{e}^{\mathbf{B}x}\,\mathbf{D}. \tag{26}$$

(2) *Non-zero steady-state distributions for inlet temperature variations*

If only temperature changes take place at inlets after the preceding process has reached a stationary state, one can find the solution vector $\mathbf{T}$ by means of the principle of superposition. In this case, thermal flow rates $\dot{W}_1$ and $\dot{W}_{2i}$ as well as heat transfer coefficients h_1 and h_{2i} are constant and the same system of governing differential equations can be used to describe both the previous steady-state process (by eliminating derivatives of temperature via time) and transient process. Assuming

$$t_m(x,z) = g_m(x) + \phi_m(x,z)$$

or

$$T_m(x,s) = g_m(x) + \Phi_m(x,s) \quad (m = 1, \mathrm{s}, 2i \text{ and } \mathrm{w}i) \tag{27}$$

one inserts them into equations (7)–(10) and the pertinent determinant conditions, bearing in mind the fact that

$$g_m(x)\left[\, g_s(x) = g_1(x) \quad \text{and} \quad g_{wi}(x) = \frac{U_{1i} g_1(x) + U_{2i} R_2 g_{2i}(x)}{U_{1i} + U_{2i} R_2} \,\right]$$

are steady-state solutions of the preceding process as $z \to \infty$. Therefore, transient parts $\phi_m(x,z)$ are described by

$$\frac{1}{Pe_1}\frac{\partial^2 \phi_1}{\partial x^2} - \frac{\partial \phi_1}{\partial x} - \frac{\partial \phi_1}{\partial z} - \sum_{i=1}^{N} U_{1i}(\phi_1 - \phi_{wi}) - U_s(\phi_1 - \phi_s) = 0 \tag{28}$$

$$\frac{1}{Pe_{2i}}\frac{\partial^2 \phi_{2i}}{\partial x^2} \pm (-1)^i \frac{\partial \phi_{2i}}{\partial x} - \varepsilon_{ci} R_\tau \frac{\partial \phi_{2i}}{\partial z} - U_{2i}(\phi_{2i} - \phi_{wi}) = 0 \quad (i = 1, 2, \ldots, N) \tag{29}$$

$$R_{wi}\frac{\partial \phi_{wi}}{\partial z} - \alpha_{1i}(\phi_1 - \phi_{wi}) - \alpha_{2i}(\phi_{2i} - \phi_{wi}) = 0 \quad (i = 1, 2, \ldots, N) \tag{30}$$

$$R_s R_w (1 + R_{c2})\frac{\partial \phi_s}{\partial z} - U_s(\phi_1 - \phi_s) = 0. \tag{31}$$

The zero initial conditions for $\phi_m(x,z)$ are

$$\phi_1(x,0) = \phi_s(x,0) = 0$$

and

$$\phi_{2i}(x,0) = \phi_{wi}(x,0) = 0 \quad (i = 1,2,\ldots,N) \quad (32)$$

and the inlet boundary conditions yields

$$\phi_1 - \frac{1}{Pe_1}\frac{\partial \phi_1}{\partial x} = f_1(z) - \left(g_1 - \frac{1}{Pe_1}\frac{dg_1}{dx}\right) \quad \text{at } x = 0$$

and

$$\frac{\partial \phi_1}{\partial x} = -\frac{dg_1}{dx} = 0 \quad \text{at } x = 1. \quad (33)$$

For flow arrangement I:

$$\phi_{21} + \frac{1}{Pe_{21}}\frac{\partial \phi_{21}}{\partial x} = f_2(z) - \left(g_{21} + \frac{1}{Pe_{21}}\frac{dg_2}{dx}\right)$$

at $x = 0$

$$\frac{\partial \phi_{2N}}{\partial x} = -\frac{dg_{2N}}{dx} = 0 \quad \text{at } x = 1 \text{ for even } N$$

or at $x = 0$ for odd N (34)

and for flow arrangement II:

$$\phi_{21} - \frac{1}{Pe_{21}}\frac{\partial \phi_{21}}{\partial x} = f_2(z) - \left(g_{21} - \frac{1}{Pe_{21}}\frac{dg_{21}}{dx}\right)$$

at $x = 0$

$$\frac{\partial \phi_{2N}}{\partial x} = -\frac{dg_{2N}}{dx} = 0 \quad \text{at } x = 0 \text{ for even } N$$

or at $x = 1$ for odd N. (35)

In general, the steady-state solution $g_1(x)$ and $g_{2i}(x)$ are determined under the following dimensionless inlet conditions

$$g_1 - \frac{1}{Pe_1}\frac{dg_1}{dx} = 1 \quad \text{at } x = 0$$

$$g_{21} + \frac{1}{Pe_{21}}\frac{dg_{21}}{dx} = 0 \quad \text{at } x = 0 \quad \text{(I)}$$

and

$$g_{21} - \frac{1}{Pe_{21}}\frac{dg_{21}}{dx} = 0 \quad \text{at } x = 1 \quad \text{(II)}.$$

Thus, the inlet conditions for $\phi_1(x,z)$ and $\phi_{2i}(x,z)$ are simplified as

$$\phi_1 - \frac{1}{Pe_1}\frac{\partial \phi_1}{\partial x} = f_1(z) - 1 \quad \text{at } x = 1 \quad (36)$$

$$\phi_{21} + \frac{1}{Pe_{21}}\frac{\partial \phi_{21}}{\partial x} = f_2(z) \quad \text{at } x = 1 \quad \text{(I)}$$

or

$$\phi_{21} - \frac{1}{Pe_{21}}\frac{\partial \phi_{21}}{\partial x} = f_2(z) \quad \text{at } x = 0 \quad \text{(II)}. \quad (37)$$

By means of the Laplace transform, one does obtain without question a homogeneous system of ordinary differential equations according to the uniform initial conditions (32). Following the afore-described procedure, one is able to find a transformed solution $\Phi_m(x,s)$ whose form is similar to equation (26), and then $T_m(x,s)$ from equation (27). In this way, the tedious task of calculating the inverse matrix $\mathbf{U}^{-1}$ is avoided.

(3) *Non-zero steady-state distributions for inlet temperature and flow rate variations*

Because of flow disturbances, thermal flow rate $\dot{W}_1$ and $\dot{W}_{2i}$ as well as heat transfer coefficients h_1 and h_{2i} are subjected to corresponding changes. The preceding treatment for pure temperature variations is not applicable. Here one should resort to expression (22) or (25). In this case, general forms of initial distributions can be expressed as

$$g_1(x) = \sum_{j=1}^{2N+2} d_j \mathbf{u}_{2N+1,j} e^{\lambda_j x}$$

and

$$g_{2n}(x) = \sum_{j=1}^{2N+2} d_j \mathbf{u}_{nj} e^{\lambda_j x} \quad (n = 1,2,\ldots,N) \quad (38)$$

where $\{\lambda_j\}$ and $\{\mathbf{u}_j\}$ are $(2N+2)$ eigenvalues and the corresponding eigenvectors, respectively. $\{d_j\}$ are $(2N+2)$ coefficients determined from the subjected boundary and interface conditions. Stationary temperature profiles in shell and tube wall are

$$g_s(x) = g_1(x)$$

and

$$g_{wi}(x) = \frac{U_{1i0}g_1(x) + U_{2i0}g_{2i}(x)}{U_{1i0} + U_{2i0}R_{20}}.$$

Henceforth, the non-homogeneous parts in equations (16)–(19) as well as in matrix equation (20) are already known. Having carried out some derivations, one finds the explicit transformed transient responses to both arbitrary temperature variations and step flow rate disturbances under the non-zero initial conditions which corresponds to the steady-state temperature distributions of a previous process

$$T_i(x,s) = \sum_{j=1}^{2N+2} d_j \mathbf{u}_{ij} e^{\beta_j x} + \sum_{m=1}^{2N+2}\sum_{k=1}^{2N+2} \mathbf{u}_{ik} v_{km} \sum_{j=1}^{2N+2} \omega_{mj} d_j \frac{e^{\lambda_j x}}{\lambda_j - \beta_k}$$

$$(i = 1,2,\ldots,2N+2) \quad (39)$$

where

$$\omega_{mj} = -Pe_{2m}\left(\varepsilon_{cm}R_c u_{mj} + \frac{U_{2m}R_{wm}}{\alpha_{1m} + \alpha_{2m} + R_{wm}s} \times \frac{U_{1m0}\mathbf{u}_{2N+1,j} + U_{2m0}R_{20}\mathbf{u}_{mj}}{U_{1m0} + U_{2m0}R_{20}}\right),$$

$$1 \leqslant m \leqslant N, \quad 1 \leqslant j \leqslant 2N+2,$$

Table 2. The interface conditions for $\phi_{2i}(x, z)$

$x = 0, \quad z \geqslant 0$	$x = 1, \quad z \geqslant 0$
$\phi_{2i} = \phi_{2i+1} = \phi_{2i,i+1}$	$\phi_{2i} = \phi_{2i+1} - \phi_{2i,i+1}$
$\frac{1}{Pe_{2i}}\frac{\partial\phi_{2i}}{\partial x} = -\frac{1}{Pe_{2i+1}}\frac{\partial\phi_{2i+1}}{\partial x}$	$\frac{1}{Pe_{2i}}\frac{\partial\phi_{2i}}{\partial x} = -\frac{1}{Pe_{2i+1}}\frac{\partial\phi_{2i+1}}{\partial x}$
even N	
I $\quad i = 1, 3, \ldots, N-1$	$i = 2, 4, \ldots, N-2$
II $\quad i = 2, 4, \ldots, N-2$	$i = 1, 3, \ldots, N-1$
odd N	
I $\quad i = 1, 3, \ldots, N-2$	$i = 2, 4, \ldots, N-1$
II $\quad i = 2, 4, \ldots, N-1$	$i = 1, 3, \ldots, N-2$

$$\omega_{2N+1,j} = -Pe_1\left[\left(1+\frac{U_s R_s R_w(1+R_{c2})}{U_s+R_s R_w(1+R_{c2})s}\right)\mathbf{u}_{2N+1,j} + \sum_{i=1}^{N}\frac{U_{1i0}\mathbf{u}_{2N+1,j}+U_{2i0}R_{20}\mathbf{u}_{ij}}{U_{1i0}+U_{2i0}R_{20}}\frac{U_{1i}R_{wi}}{\alpha_{1i}+\alpha_{2i}+R_{wi}s}\right], \quad 1 \leqslant j \leqslant 2N+2$$

$\omega_{mj} = 0$ for other m and $1 \leqslant j \leqslant 2N+2$.

4. TRANSIENT RESPONSE

The inversion of the Laplace transform must be performed to obtain real-time transient responses of heat exchangers from the afore-derived solutions in the image-domain. It is almost impossible to carry out analytical inversion of transformed solutions (25) or (39) and one should resort to techniques of numerical inversion. Two numerical algorithms have been used to calculate transient temperature profiles and tube heat exchangers [10, 12]. One is called the Gaver–Stehfest algorithm and the other uses Fourier series approximation. For the sake of consistence, they are transcribed as follows:

(1) Gaver–Stehfest algorithm [13]

$$f(z) = \frac{\ln 2}{z}\sum_{m=1}^{M} K_m F\left(m\frac{\ln 2}{z}\right) \quad (M \text{ must be even})$$

$$K_m = (-1)^{m+M/2} \times \sum_{k=[(m+1)/2]}^{\min(m,M/2)} \frac{k^{M/2}(2k)!}{(M/2-k)!k!(k-1)!(m-k)!(2k-m)!}. \tag{40}$$

(2) Numerical inversion based on Fourier series [14]

$$f(z) = \frac{e^{az}}{z}\left[\frac{1}{2}f(a) + Re\sum_{k=1}^{r} F\left(a+\frac{ik\pi}{z}\right)(-1)^k\right]. \tag{41}$$

Constant a is generally chosen in the range $4 < az < 5$, so that the truncation error can be considered to be small enough. As pointed out in the previous work, the first algorithm needs much less computation time than the second does, but it may fail to predict transient responses to inlet changes with oscillatory components. In this case the second algorithm is more suitable. According to the type of given inlet variations, either of these two algorithms is selected to determine transient behaviour of heat exchangers. The inverse results as $z \to \infty$ correspond to steady-state temperature distributions.

5. EXAMPLES AND DISCUSSIONS

By means of the numerical algorithms of inversion, one can promptly find transient temperature profiles, no matter whether the initial conditions are uniform or not and no matter how complicated the transformed solution is. In order to show the application of the above-developed method, some examples are illustrated in Figs. 2–4 under parameters $R_r = 1$, $U_1 = U_2$, $R_s = 0.2$ and $coef = 0.1$. Figure 2 describes the shellside temperature distribution $t_1(x, z)$ subject to a step temperature change in a counterflow exchanger. The curved surface in the diagram evidently shows how the temperature wave propagates from the inlet to the exit (from the high to the low).

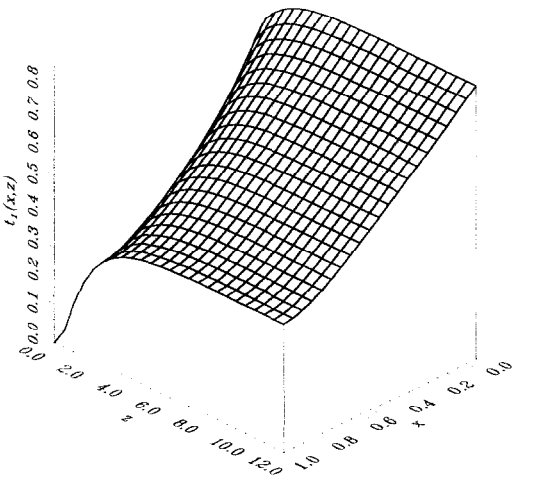

FIG. 2. Shellside temperature distribution $t_2(x, z)$ subject to a step temperature variation in a counterflow heat exchanger ($R_1 = 1$, $R_w = 0.4$, $NTU_1 = 2.5$, $Pe_1 = 4$, $Pe_2 = 10$, $\sigma_1 = \sigma_2 = 1$, $f_1(z) = 1$ and $f_2(z) = 0$).

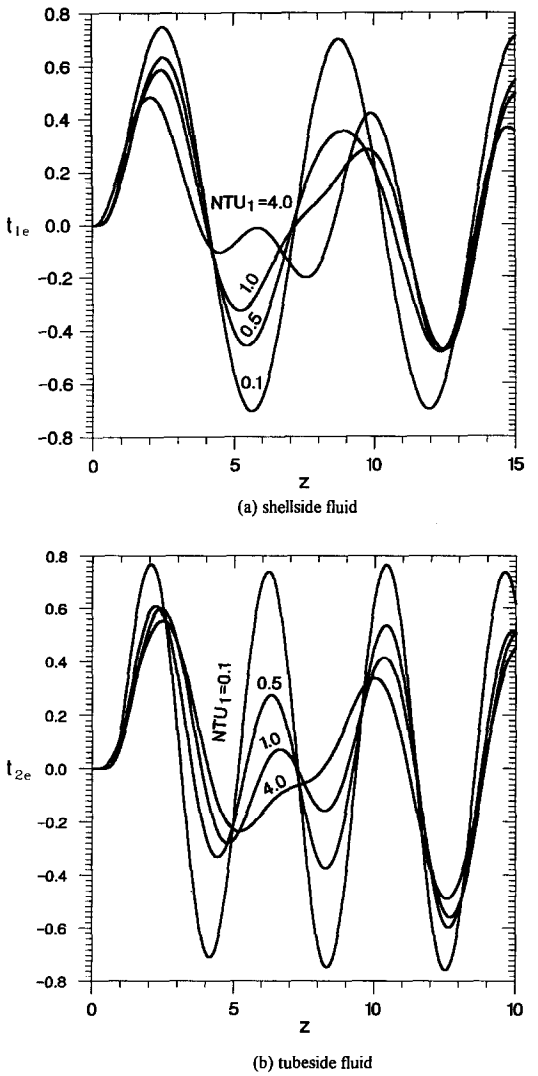

FIG. 3. Superposition of exit responses to periodic inlet temperatures $f_1(z) = \sin z$ and $f_2(z) = \sin 1.5z$ in a 1–2 heat exchanger with flow arrangement I ($\varepsilon_{11} = \varepsilon_{12} = 0.5$, $\varepsilon_{21} = \varepsilon_{22} = 0.5$, $\varepsilon_{c1} = \varepsilon_{c2} = 0.5$, $\varepsilon_{w1} = \varepsilon_{w2} = 0.5$, $R_1 = 1$, $R_w = 0.6$, $Pe_1 = 4$, $Pe_{21} = Pe_{22} = 10$, $\sigma_1 = \sigma_2 = 1$). (a) Shellside fluid; (b) tubeside fluid.

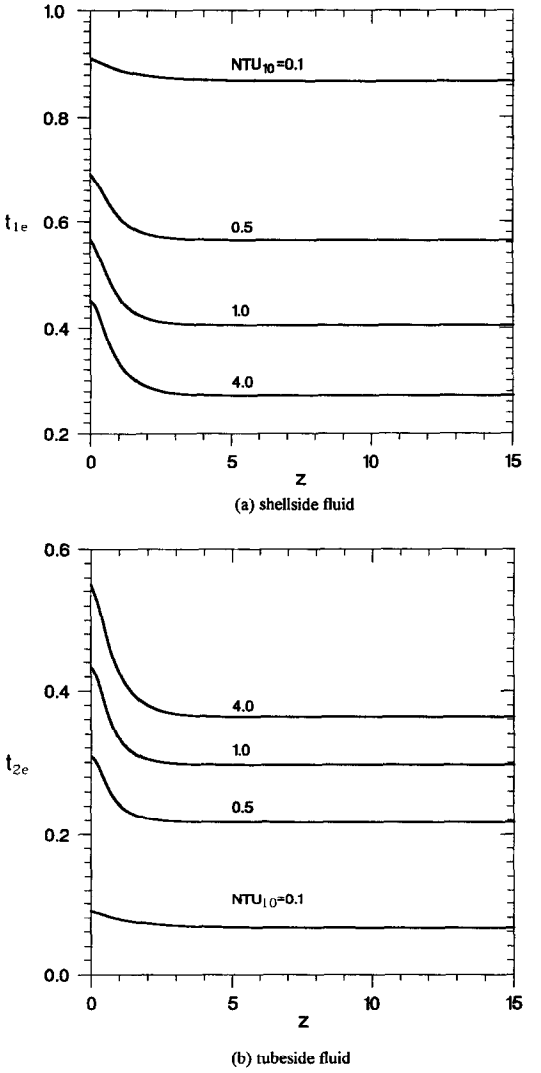

FIG. 4. Exit responses to step disturbances of flow rates in a 1–4 heat exchanger with flow arrangement II ($\varepsilon_{11} = \varepsilon_{12} = \varepsilon_{13} = \varepsilon_{14} = 0.25$, $\varepsilon_{21} = \varepsilon_{22} = \varepsilon_{23} = \varepsilon_{24} = 0.25$, $\varepsilon_{c1} = \varepsilon_{c2} = \varepsilon_{c3} = \varepsilon_{c4} = 0.25$, $\varepsilon_{w1} = \varepsilon_{w2} = \varepsilon_{w3} = \varepsilon_{w4} = 0.25$, $R_{10} = 1$, $R_w = 0.4$, $Pe_1 = 6$, $Pe_{21} = Pe_{22} = Pe_{23} = Pe_{24} = 8$, $\sigma_1 = 0.6$, $\sigma_2 = 1.2$, $f_1(z) = 1$ and $f_2(z) = 0$). (a) Shellside fluid; (b) tubeside fluid.

The temperature steeply increases in the range $z < 3$ and the performance approaches a stationary state for $z > 10$. The slope of profile $t_1(x, z)$ depends mainly upon R_1, NTU_1, and Péclet numbers.

Figure 3 introduces an example in which two sine temperature waves $f_1(z) = \sin z$ and $f_2(z) = \sin 1.5z$ are respectively generated at the shell and tubeside inlets of an exchanger with two tube passes. The shellside response at the exit is shown in Fig. 3(a) and the tubeside response in Fig. 3(b). The remarkable attenuation and superposition of two temperature waves take place for greater values of NTU_1, especially for $NTU_1 > 1$. In such cases the interference of two waves with different periods may greatly cut down the amplitude of the synthesised wave. The curves show that the damping function of both fluids and tube wall depends upon not only values of heat capacities but also the value of NTU_1. The damping increases with greater NTU_1 and the amplitude at the exit becomes lower. The effect of the shell on transient process has the similar feature, too. In brief, one should distinguish the effect of such solid components as tube and shell on transient behaviour according to both values of heat capacities and heat transfer coefficients between these components and fluids.

An example of step disturbances of flow rates ($\sigma_1 = 0.6$ and $\sigma_2 = 1.2$) is plotted in Fig. 4. In this example the non-zero initial conditions are identical to the steady-state temperature distributions of the previous process. The curves in Figs. 4(a) and (b)

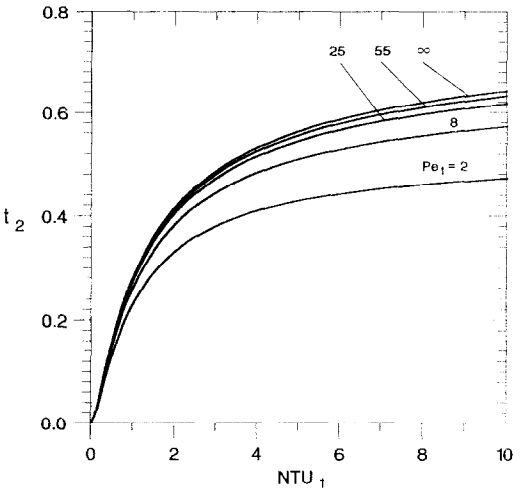

FIG. 5. Effect of the Péclet number Pe_1 on transient behaviour in a counterflow heat exchanger ($R_1 = 0.8$, $R_w = 0.3$, $Pe_1 = 2$, $Pe_2 = 60$, $\sigma_1 = \sigma_2 = 1$, $f_1(z) = 1$ and $f_2(z) = 0$).

represent the shell and tubeside exit responses of an exchanger with four tube passes in flow arrangement II. The value of t_{2e} or t_{1e} at $z = 0$ corresponds to thermal effectiveness of the previous process. These curves show that a decrease of shellside flow rate causes reduction of exit temperatures and that this reduction becomes more considerable for $NTU_1 > 0.1$, as expected. Obviously, the transient process resulting from step disturbance of flow rates already approaches a new stationary state for $z > 8$. Both Figs. 4(a) and (b) show an accurate energy balance ($R_1(1-t_{1e}) = t_{2e}$ for $z > 10$) between shell and tubeside fluids at the steady state, which provides a proof that the afore-derived method is feasible to predict transient behaviour of multipass shell and tube heat exchangers.

As previously pointed out, maldistribution incurs degeneration of thermal performance of exchangers and the measure of flow maldistribution is the Péclet number (here Pe_1 and Pe_{2i}). Figure 5 illustrates tubeside exit temperature at $z = 1.5$ vs NTU_1 corresponding to different values of Pe_1 and shows how the maldistribution exerts its influence on transient behaviour. The quantitative description in Fig. 5 reveals that the effect of maldistribution is considerably strong if $Pe_1 < 25$ and this effect increases with increasing NTU_1. With regard to possible maldistribution, designers must provide exchangers with a higher value of NTU and measures against the occurrence of maldistribution to reach the specified effectiveness. On the other hand, the effect of maldistribution is negligible if $Pe_1 > 55$. In fact, the dispersion model is almost identical to the conventional plug-flow model for $Pe > 55$. In other words, application of the dispersion model is of importance for smaller Pe_1, especially for $Pe_1 < 25$. It is predicted that the effect of Pe_{2i} is identical to that of Pe_1. For tubeside laminar flow, the effect of maldistribution becomes more evident and application of the dispersion model to tubeside fluid is of greater meaning.

Setting $N = 1$, one finds that forms of dimensionless governing equations (7)–(10) are similar to those describing heat exchange process in fixed-matrix or rotary regenerators. Therefore, the method developed in this paper can be used to determine temperature profiles and thermal effectiveness of regenerators. There the value of NTU is normally considerably great ($NTU > 10$) and the effect of maldistribution becomes more intensive if flow maldistribution occurs, and then the dispersion model will be more suitable and more powerful than the conventional plug-flow model.

6. CONCLUSIONS

Based on the dispersion model rather than the ideal plug-flow model, an efficient and versatile method of predicting transient behaviour of multipass shell and tube heat exchangers has been developed. Taking the effect of shell and tubeside flow maldistribution and the influence of heat capacities of fluids as well as solid components such as shell, tube wall, baffles and end plates into account, the method can handle transient responses to arbitrary temperature variations and step disturbances of flow rates which may occur simultaneously or separately and on either or both sides. Three typical types of initial conditions have been discussed in detail. According to the type of the given initial conditions, one can choose a simple and convenient calculation procedure. The Laplace transform has been used to carry out simulation of heat process. In order to obtain the final solution in real time-domain, the numerical inversion of the Laplace transform has been applied. Two different algorithms have been introduced. One should select either of them in correspondence with types of inlet variations to determine transient responses accurately and promptly.

Flow maldistribution hinders transient responses to any inlet changes and decreases thermal effectiveness of heat exchangers. Its effect becomes more remarkable with increasing NTU. The Péclet number has been used to quantitatively describe this kind of effect. The calculation has shown that the dispersion model should be applied instead of the plug-flow model if $Pe < 55$.

Acknowledgement—The authors would like to thank the 'Deutsche Forschungsgemeinschaft' for the financial support of this research project.

REFERENCES

1. F. E. Romie, Transient response of the parallel-flow heat exchanger, *J. Heat Transfer* **107**, 727–730 (1985).
2. D. J. Correa and J. L. Marchetti, Dynamic simulation of shell-and-tube heat exchangers, *Heat Transfer Engng* **8**, 50–59 (1987).
3. H. M. Paynter and Y. Takahashi, A new method of

evaluating dynamic response of counterflow and parallel-flow heat exchangers, *Trans. ASME* **78,** 749–758 (1956).
4. D. J. Yang, Transient heat transfer in a vapor-heated heat exchanger with arbitrary timewise variant flow perturbation, *J. Heat Transfer* **64,** 133–142 (1964).
5. F. P. Stainthorp and A. G. Axon, The dynamic behaviour of a multipass steam-heated heat exchanger—I. Response to steam temperature and steam flow perturbations, *Chem. Engng Sci.* **20,** 107–119 (1965).
6. R. Forgieri and G. Papa, Dynamic response of countercurrent heat exchangers to temperature disturbances and step flow variations, *Proc. of the Sixth Int. Heat Transfer Conf.*, Toronto, Vol. 8, HX-18 (1978).
7. Y. Xuan and W. Roetzel, Dynamics of shell-and-tube heat exchangers to arbitrary temperature and step flow variations, *A.I.Ch.E. Jl* **39**(3), 413–421 (1993).
8. T. Tinker, Shell side characteristics of segmentally baffled shell-and-tube heat exchangers, Part I, II and III, *Proc. General Discussion on Heat Transfer*, pp. 89–116. IMechE, London (1951).
9. W. Roetzel and Y. Xuan, The effect of core longitudinal heat conduction on the transient behaviour of multipass shell and tube heat exchangers, *Heat Transfer Engng* **14**(1), 52–61 (1993).
10. W. Roetzel and Y. Xuan, Transient behaviour of multipass shell-and-tube heat exchangers, *Int. J. Heat Mass Transfer* **35,** 703–710 (1992).
11. J. C. Mecklenburgh and S. Hartland, *The Theory of Backmixing*. Wiley, London (1975).
12. W. Roetzel and Y. Xuan, Transient response of parallel and counterflow heat exchangers, *J. Heat Transfer* **114,** 510–512 (1992).
13. H. Stehfest, Numerical inversion of Laplace transforms. *Commun. ACM* **13,** 47–49 (1970).
14. S. Ichikawa and A. Kishima, Application of Fourier series technique to inverse Laplace transform, *Kyoto Univ. Memoires* **34,** 53–67 (1972).